Influence of optical wavelength on terahertz radiation from laser-induced air plasma

Siqing Wu (吴四清)[1,2], Jinsong Liu (刘劲松)[1*], Shenglie Wang (汪盛烈)[1], and Yanan Zeng (曾延安)[1]

[1] *Wuhan National Laboratory for Optoelectronics, School of Optical and Electronic Information, Huazhong University of Science and Technology, Wuhan 430074, China*

[2] *School of Electronic and Information Engineering, Hubei University of Science and Technology, Xianning 437100, China*

[*] *Corresponding author: jsliu4508@vip.sina.com*

Received May 15, 2013; accepted September 4, 2013; posted online September 30, 2013

Using a well-developed transient photocurrent model, we combine theoretical and numerical studies on the production of terahertz (THz) radiation in laser-induced air plasma. Air molecules are excited and then ionized by the laser-pulses mixing the fundamental and second harmonic fields. As a result, a non-vanishing directional photoelectron current emerges, radiating the THz pulse wave. We mainly discuss the influences of optical wavelength on THz radiation in five different cases. Results show that the fundamental-pulse width (50 fs), energy, and relative phase between two pulses are invariant. When the laser wavelength (from 400 nm to 1.25 μm) becomes longer, the emitted THz fields are significantly enhanced, with a linear dependence on the optical wavelength.

OCIS codes: 140.3440, 190.7110, 320.2250, 260.7120.
doi: 10.3788/COL201311.101402.

By focusing a strong laser beam into ambient air, Hamster *et al.* firstly achieved the generation of terahertz (THz) radiation in laser-induced gas plasma in the early 1990s[1,2]. Since then, using gas in generating THz wave has elicited considerable attention[1−6]. The potential for nonlinear THz optics and spectroscopy, THz pump probe experiments, as well as biomedical and security imaging, has driven studies on generating THz[7]. In the intrinsic process of generating THz, the focused laser excites and ionizes the gas by stripping off bound electrons from the parent molecules. Ionized electrons are then accelerated by the laser ponderomotive force. As a result, electromagnetic waves, including THz components, are eradiated in the far field. To improve THz radiation intensity, Löffler *et al.*[8,9] applied an external direct current (DC) bias across the ionized gas region, which caused a least order-of-magnitude increase in the THz field strength. However, given the screening effect of the applied bias, further enhancement of the THz field is difficult by utilizing the above method. As an alternative scheme[10], a two-color laser mixture of a fundamental (ω) wave and a second harmonic (2ω) is employed instead of the single-color optical beam. Nearly 40-fold enlargement can be achieved for the enhancement of THz field compared with the case for single color[11]. The phenomenon is mainly attributed to the disappearance of screening effect, which is caused by the greater frequency of the laser field than the plasma. Kim *et al.* introduced a transient photo current (PC) mode which indicated that plasma is responsible for THz wave generation[12,13]. The above mentioned research explained the underlying physical mechanism of THz wave generation.

Numerous theoretical and experimental studies have been conducted on the generation of THz waves from two-color, laser-excited air plasma[11−19]. However, the influence of optical wavelength on THz radiation has not been studied in detail. In this letter, we focused on the influence of optical wavelength on THz radiation in theories and calculations using the transient PC model.

Under the effect of intense laser, the physical pattern of air molecule photoionization has few hierarchies depending on the optical intensity[20,21]. At lower laser intensity ($I \leqslant 10^{14}$ W/cm^2, $E \leqslant 10^{10}$ V/m), multiphoton-ionization (MPI) is dominant; otherwise, tunneling ionization (TI) emerges. A value $\gamma=\sqrt{I_\mathrm{p}/(2U_\mathrm{p})}$ is used to judge the suitable model. In this study, I_p is the ionization potential and $U_\mathrm{p} = e^2E^2/(4m\omega^2)$ is the ponderomotive energy, which is the average kinetic energy of a free electron in a laser field with amplitude E and frequency ω. The transition status between MPI and tunneling ionization is $\gamma = 1$. At higher optical intensity ($\gamma \ll 1$), ionization is dominated by TI. In the simulations, laser intensity is estimated to be more than 10^{14} W/cm^2, the ionization potential of N_2 (the main component of air) is $I_p = 15.576$ eV, and the ponderomotive energy is $U_P = 59.7$ eV. The calculated γ is $0.3612 < 1$, indicating that the TI model is appropriate.

For tunneling ionization, the ionization rate can be described as [23]

$$w(t) = 4w_0\frac{E_\mathrm{a}}{E(t)}\left(\frac{E_\mathrm{i}}{E_\mathrm{h}}\right)^{5/2}\exp\left[-\frac{2}{3}\frac{E_\mathrm{a}}{E(t)}\left(\frac{E_\mathrm{i}}{E_\mathrm{h}}\right)^{3/2}\right], \tag{1}$$

where $w_0 = \kappa^2me^4/\hbar^3 \approx 4.13\times10^{16}\,\mathrm{s}^{-1}$ is the atomic frequency unit ($\kappa = 1/(4\pi\varepsilon_0)$; m is the electron mass; e is the charge; $E_\mathrm{h} \approx 13.6$ eV is the ionization potential of hydrogen; $E_\mathrm{i} \approx 15.6$ eV is the ionization potential of N_2 (the main constituent of air); $E_\mathrm{a} = \kappa^3m^2e^5/\hbar^4 \approx 5.14\times10^{11}$ V/m is the atomic unit of electric field; and $E(t)$ is the amplitude of the employed laser field.

Based on the ionization rate $w(t)$, plasma density $\rho(t)$

can be obtained using[21]

$$\frac{\partial \rho(t)}{\partial t} = w(t)[\rho_0 - \rho(t)], \tag{2}$$

where ρ_0 is the gas initial density. Once ionized, the freed electrons undergo a force from the optical field and disseminate as classical particles. The electron velocity at time t is computed as

$$v(t) = -(e/m)\int_{t_0}^{t} E(t')\mathrm{d}t', \tag{3}$$

where t_0 is the instant when the electron is liberated. Collision processes during the laser pulse are not considered. In tunneling ionization, the ionized electrons are presumed motionless at the ionization moment t_0, i.e., $v(t_0) = 0$. The resulting transverse electron current can be described as[12]

$$J(t) = \int_{t_0}^{t} ev(t,t')\rho_{\mathrm{e}}(t')\mathrm{d}t', \tag{4}$$

where $v(t,t')$ is the velocity at time t of electrons that emerged at t'; $\rho_{\mathrm{e}}(t') = w(t')[\rho_0 - \rho(t')]$ is the varying rate of the plasma density at t'; $ev(t,t')\rho_{\mathrm{e}}(t')\mathrm{d}t'$ is the contribution of the ionized electrons at time $t' \sim (t' + \mathrm{d}t')$ to the electron current at a subsequent time t.

The employed optical field can be expressed as

$$E(t) = \frac{1}{2}E_{\omega 0}\exp(-t^2/T_{\omega 0})\mathrm{e}^{\mathrm{i}\omega t} + \frac{1}{2}E_{2\omega 0}\exp(-t^2/T_{2\omega 0})\mathrm{e}^{\mathrm{i}(2\omega t+\theta)}, \tag{5}$$

where ω and 2ω are the laser frequencies and $E_{\omega 0}$ and $E_{2\omega 0}$ are the peak amplitudes. The field E_0 can be obtained via $E_0 = (2/\pi)^{3/4}(2W/\varepsilon c T_0)^{1/2}\big/\phi$, where ε, c, and ϕ are gas medium permittivity, light speed, and laser beam radius, respectively, which is based on optical energy W. The pulse widths are $T_{\omega 0}$ and $T_{2\omega 0}$ $(= T_{\omega 0}/\sqrt{2})$, where $T_{\omega 0}$ can be obtained via $T_{\omega 0}$=$T_{\mathrm{FWHM}}/\sqrt{2\ln 2}$. T_{FWHM} is the full-width at half-maximum (FWHM) and θ is the relative phase between two optical pulses.

The laser pulse is selected at the fundamental pulse duration $T_{\omega 0}$= 50 fs, and the relative phase is set at $\theta = \pi/2$ for acquiring the largest THz yield[13]. The laser pulse energy is fixed at 300 μJ. The ratio of pulse energy is distributed as 80% (fundamental) and 20% (harmonic). The laser beam radius is estimated at ϕ=10 μm. Five cases with different fundamental wavelengths (λ), namely, 400 nm, 600 nm, 800 nm, 1.0 μm and 1.2 μm, are discussed in detail.

Under the influence of the laser electric field, the ionized electrons are accelerated along the field direction and generate an electron current J(t). The electron current is determined by solving Eq. (4). The results are shown in Fig. 1. Transport and space charge effects are ignored in Eq. (4). Simultaneously, the collision process of the electron–ion and electron–neutral is not taken into account for simplicity. Adding fundamental laser wavelength can greatly strengthen the electron current (Fig. 1). Besides the oscillatory feature, a non-zero DC electron current also appears after the laser pulse disappears, which eradiates THz emission in the far field.

Computing the derivative of $J(t)$ at time t, we can obtain a time-varying THz field. The THz waveforms for the five specific cases are plotted in Fig. 2. The final THz emission exhibits a remarkable increase under the following conditions: (a) pulse wavelength increases; (b) irradiating laser pulse width is maintained; (c) relative phase and laser energy are invariant. The result can be ascribed to the increase in laser wavelength. Given the increased laser wavelength, the number of laser cycles needed to ionize the gas is reduced. As a result, higher asymmetry of the ionization triggers stronger net ionizing currents and more powerful THz radiation. Figure 2 also shows that THz waveforms under the five cases are changeless, indicating that the increase of laser wavelength does not cause the THz spectrum to vary.

The THz electromagnetic spectra can be obtained using Fourier transform. Figure 3 shows the corresponding spectra graph for the five cases. The waveform of the spectra has no variation, except for the enlargement of amplitudes with increasing optical wavelength. The result agrees with the above analysis. The spectra amplitudes are nearly equal to zero at greater frequency

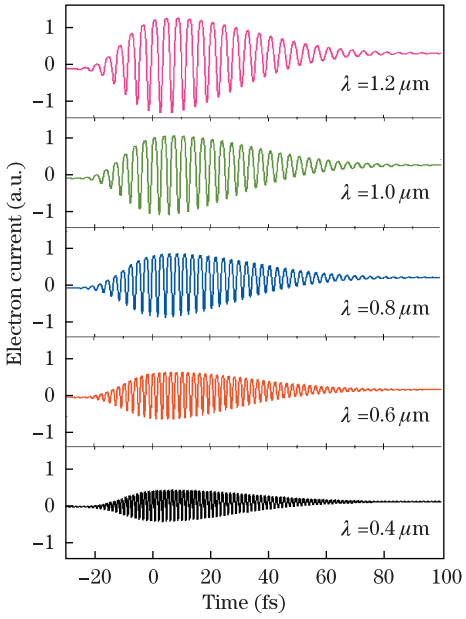

Fig. 1. (Color online) Time-varying electron current under different fundamental laser wavelengths.

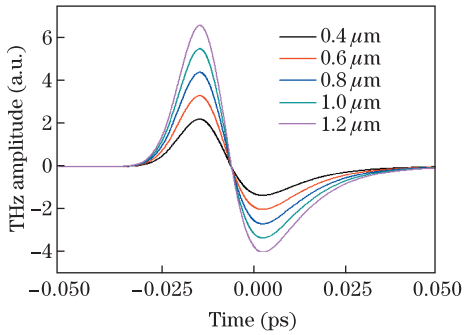

Fig. 2. (Color online) THz waveforms obtained with 150-THz low-pass filtering under different fundamental laser wavelengths.

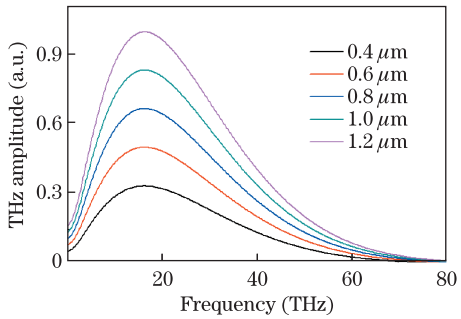

Fig. 3. (Color online) The corresponding THz radiation spectra under different fundamental laser wavelengths.

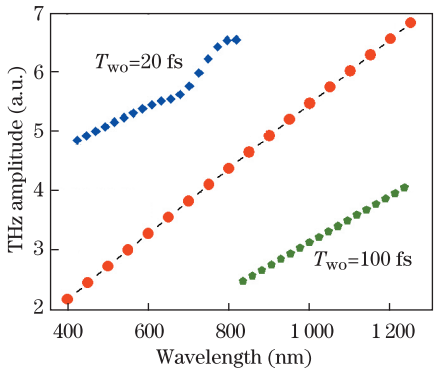

Fig. 4. (Color online) THz amplitude versus the fundamental laser wavelength at $T_{\omega 0}$=50 fs.

range (>80 THz), which is mainly caused by the declining edge of the selected low-pass filter in the calculation.

The dependent relationship of THz amplitude on the driving field wavelength is computed as the fundamental optical wavelength that is discretely changed from 400 nm to 1.25 μm. The step is fixed at 50 nm. Figure 4 shows the calculated finding. When the fundamental wavelength becomes longer, THz emissions can be linearly enhanced in the considered wavelength range. A similar result wherein the mid-infrared pump pulse is used as the driving source was verified experimentally in Ref. [23]. We also calculated the other two cases, wherein the fundamental pulse duration was set at $T_{\omega 0}$=20 and 100 fs. The inset in Fig. 4 shows the results. From the two insets, the THz emission is scaled with the laser wavelength at $T_{\omega 0}$=100 fs. However, the situation is slightly different at $T_{\omega 0}$=20 fs. Only single ionization is taken into account in the simulations. Our calculations show that double ionization nearly takes place simultaneously with single ionization. However, as the laser energy reaches 300 μJ, the double ionization rate becomes smaller relative to single ionization. The contribution from the double ionization to THz generation can almost be ignored.

In conclusion, the transient PC model is used to simulate the physical process of engendering THz emission in air plasma, which was excited by a two-color pulsed laser mixing fundamental ω and second harmonic 2ω pulses. We focuse on the dependence of THz field in the incident fundamental laser wavelength. Five cases of optical wavelength at 400 nm, 600 nm, 800 nm, 1.0 μm, and 1.2 μm are also discussed. Results show that increasing the incident laser pulses wavelength can significantly strengthen the output THz peak field amplitude. However, no change occurs at the THz spectrum component. The dependency of THz field on the optical wavelength is computed by selecting 18 discrete values. The corresponding curves are plotted in the figures.

This work was supported by the National Natural Science Foundation of China (No. 61177095), the Hubei Natural Science Foundation (No. 2012FFA074), the Ph. D. Program Foundation of the Ministry of Education of China (No. 20100142110042), and the Fundamental Research Funds for the Central Universities (Nos. 2012QN094 and 2012QN097).

References

1. H. Hamster, A. Sullivan, S. Gordon, W. White, and R. W. Falcone, Phys. Rev. Lett. **71,** 2725 (1993).
2. H. Hamster, A. Sullivan, S. Gordon, and R. W. Falcone, Phys. Rev. E **49,** 671 (1994).
3. T. Bartel, P. Gaal, K. Reimann, M. Woerner, and T. Elsaesser, Opt. Lett. **30,** 2805 (2005).
4. K. Y. Kim, A. J. Taylor, J. H. Glownia, and G. Rodriguez, Nat. Photon. **2,** 605 (2008).
5. X. Zhang and J. Xu, *Introduction to THz Wave Photonics* (Springer, Berlin, 2009).
6. W. Wang, Z. Sheng, Y. Li, L. Chen, Q. Dong, X. Lu, J. Ma, and J. Zhang, Chin. Opt. Lett. **9,** 110002 (2011).
7. M. S. Sherwin, C. A. Schmuttenmaer, and P. H. Bucksbaum, http://www.er.doe.gov/bes/reports/files/THz_rpt.pdf (2004).
8. T. Löffler, F. Jacob, and H. G. Roskos, Appl. Phys. Lett. **77,** 453 (2000).
9. T. Löffler and H. G. Roskos, J. Appl. Phys. **91,** 2611 (2002).
10. D. J. Cook and R. M. Hochstrasser, Opt. Lett. **25,** 1210 (2000).
11. X. Xie, J. Dai, M. Yamaguchi, and X. Zhang, Proc. SPIE **6212**, 62120N (2006).
12. K. Y. Kim, J. H. Glownia, A. J. Taylor, and G. Rodriguez, Opt. Express **15,** 4577 (2007).
13. K. Y. Kim, Phys. Plasmas **16,** 056706 (2009).
14. M. Kress, T. Löffler, S. Eden, M. Thomson, and H. G. Roskos, Opt. Lett. **29,** 1120 (2004).
15. X. Xie, J. Dai, and X. Zhang, Phys. Rev. Lett. **96,** 075005 (2006).
16. N. Karpowicz and X. Zhang, Phys. Rev. Lett. **102,** 093001 (2009).
17. J. Dai, N. Karpowicz, and X. Zhang, Phys. Rev. Lett. **103,** 023001 (2009).
18. H. Wen and A. M. Lindenberg, Phys. Rev. Lett. **103,** 023902 (2009).
19. G. Rodriguez and G. L. Dakovski, Opt. Express **18,** 15130 (2010).
20. D. W. Schumacher and P. H. Bucksbaum, Phys. Rev. A **54,** 4271 (1996).
21. M. D. Thomson, M. Kreß, T. Löffler, and H. G. Roskos, Laser Photon. Rev. **1,** 349 (2007).
22. N. B. Delone and V. P. Krainov, *Atoms in Strong Light Fields* (Springer-Verlag, Berlin, 1985).
23. M. Clerici, M. Peccianti, B. E. Schmidt, L. Caspani, M. Shalaby, M. Giguère, A. Lotti, A. Couairon, F. Légaré, T. Ozaki, D. Faccio, and R. Morandotti, arXiv **1207**, 4754 (2012).